CGU HS Committee on River Ice Processes and the Environment
19th Workshop on the Hydraulics of Ice Covered Rivers
Whitehorse, Yukon, Canada, July 9-12, 2017.

3D side scan sonar imaging of in-situ anchor ice in the Peace River

Joel Evans[1], Martin Jasek[1], Kerry Paslawski[2], and Paul Kraeutner[3]

[1]BC Hydro, 6911 Southpoint Drive, Burnaby, B.C., Canada, V3N 4X8
joel.evans@bchydro.com, martin.jasek@bchydro.com

[2]Timberoot Environmental, RR1 Site 7 Box 43, Beaverlodge, AB, T0H 0C0
kerry.timberoot@gmail.com

[3]Ping Digital Signal Processing Inc., 10990 Madrona Drive, North Saanich, B.C., V8L 5R7
paul@pingdsp.com

Anchor ice (AI) has been measured, studied, and photographed by others for decades. AI formation and release causes fluctuations in discharge and water level in rivers both while it forms and when it releases (AI waves). This paper presents new data, gathered using side scan sonar and swath bathymetry, to further the understanding of these AI waves and the anchor ice lifecycle in a reach of the Peace River in Alberta, Canada. This may help improve river ice models to better manage hydropower production and the risk of freeze-up ice jam flooding at the Town of Peace River, Alberta.

Data was collected on six trips along the same 13 km reach of the river including two when the water was super cooled and anchor ice was forming on the river bed, two when anchor ice was present but water had just warmed above the freezing point, one where almost all the AI was gone and one when the water was well above freezing and the river bed was completely free of ice.

The side scan sonar instrument provided data to quantify the anchor ice on a large deep river where AI cannot be measured directly as has traditionally been done in smaller streams. The data may be used to validate and add to the current body of knowledge surrounding anchor ice in large rivers, and to confirm calculations of the spatial extents of anchor ice formation, changes in hydraulic roughness, and the computed thickness of anchor ice in river ice models.

1. Introduction and background

Many parameters affecting anchor ice (AI) formation and release are site specific, likely varying spatially and temporally within the same river. Visual observation of in-situ AI on the Peace River is not routinely possible due to the depth and turbidity of the water. However, the effects of AI formation and release are often observed and include flow fluctuations due to ice storage and release, increases in river stage due to ice accretion, and changes in hydraulic roughness.

To date, direct and indirect observations and measurements of AI on the Peace River have been limited to: stage measurement at many locations (Jasek et al, 2015), flow measurement with an ADCP (Jasek, 2016), stationary and mobile deployment of a 1D shallow water ice profiling sonar (Marko et al, 2017), some opportunistic photos and videos during atypical flow reductions at the upstream hydroelectric dam (Jasek et al, 2015) and many observations of anchor ice after it has released and floated to the surface.

The plan for this iteration of data collection is to use swath imagery from a side scan sonar, and bathymetric data, to observe and document the evolution of in-situ AI along a stretch of the Peace River. The equipment that is used is a 3D side scan sonar from Ping DSP Inc. in North Saanich, BC, Canada. Their pole-mount sonar instrument collects traditional 2D side scan imagery at 450 kHz. It also uses patented technology to produce swath bathymetry and 3D side scan imagery. Its swath bathymetry, even in shallow water, can be of survey quality when collected using GPS equipment that has sufficient accuracy.

2. Methodology, river reach description and relevant environmental data

To collect data on the Peace River, the sonar instrument was mounted on a vertical pole and affixed to the side of a zodiac-style inflatable boat. The pole allowed vertical adjustment of the sonar so that it could be as high as possible in the water column without having its beams obstructed by adjacent frazil pans and rafts. A submersible RBRsolo T temperature logger with ± 0.002 °C accuracy was also attached to the pole next to the sonar. The boat and sonar equipment are shown in Figure 1.

At this early stage of data collection, the GPS equipment that was used was not of sufficient accuracy to produce survey-quality bathymetry. Collecting data along a longer stretch of the river was deemed more important than higher accuracy over a smaller area. The relative accuracy of the 3D imagery and bathymetry was still of survey quality, however the reference location of the boat was not known with high accuracy. Instead, a 10-Hz marine GPS with accuracy of 3 m was used.

The study location was near Dunvegan, Alberta and in the context of North America, is shown in Figure 2. The stretch of the Peace River that was imaged extends from the Dunvegan highway bridge down to the Fairview water intake – approximately 13 km in length (Figure 3). This is about 300 km downstream of BC Hydro's Peace Canyon dam and about 100 km upstream of the Town of Peace River, Alberta.

At the time of data collection, the studied reach of the Peace River was 1 – 7 m deep and varied between 220 m and 440 m in width. Flow velocity was approximately 1 – 3 m/s.

Both traditional 2D side scan imagery and 3D bathymetry and imagery was collected for a 100 m swath of river along this reach. This reach of river was surveyed six times in early 2017 under different weather and AI conditions. Each survey trip down the river is referred to as a float trip or a “float” because the direction of travel was in the same direction as the river current. Only a small electric trolling motor used for small course corrections in order to follow approximately the same GPS track as previous floats. This allowed the six tracks to be within about 20 m of each other most of the time. The bed profile in the centre of this swath for all six traversals is shown in Figure 4, and Figure 5 shows a magnified portion in a reach with a broad gravel bar. More concentrated river ice floes in narrower reaches and on heavier ice floe days made it challenging to maintain heading and wooden poles were useful in pushing ice floes out of the way to follow the proper course (Figure 1c).

Figure 6 shows the variations in river stage, river flow, water temperature, and air temperature at the Dunvegan highway bridge throughout the winter of 2017, including those during the six floats. It also includes the flow release into the river 300 km upstream from the Peace Canyon dam, which is operated by BC Hydro. Inflows from tributaries along the 300 km stretch are typically less than 10% of the total river flow rate, quasi steady, and on a slow winter recession. In Figure 7, the same graphs are expanded to show the hydraulic and environmental conditions in more detail during the first four floats, when AI was observed. The last two floats were in March and intentionally occurred when little or no AI was expected to be present. It should also be noted that the steep increases in river stage in March in Figure 6 are due to the approaching ice front and corresponding backwater effects at the river gauge. This backwater is also apparent in the water surface profiles for March 14 and 15 in Figure 4 where the depth is approximately doubled compared to the February floats and the slope of the water surface is only a small fraction of the normal river bed slope in this reach.

3. Results

A phenomenon that is not evident in the water temperatures in Figures 6 and 7, but that shows up in river ice modeling, is the 0 °C isotherm, which moves along the river many tens, or even a hundred kilometers or more on some days due to diurnal heating/cooling and solar energy input. During the float on February 7, the high accuracy temperature probe mounted to the sonar indicated that some areas of the studied river reach were above freezing while most of the reach was below freezing (Figure 8). On that day, the air temperatures peaked at -13 °C. These above freezing water temperatures could be contributing to partial AI release and may also limit overall AI accretion in contrast to the larger January episode of AI buildup (Figure 7a) when the sun angle was lower and the diurnal temperature fluctuations (Figure 7b) were less pronounced.

Figure 8 also shows the water temperatures as measured next to the sonar instrument for the other three floats that contained a large amount of AI. On both February 11 and 12 the water temperatures were above freezing for almost the entire float even though AI was visibly covering much of the river bed. Water temperatures during the floats on March 14 and 15 were not included in this graph because they were 0.1 °C and 0.9 °C respectively – well above freezing. Only a small amount of AI on the river bed was present on the March 14 float, and no AI was observed on the March 15 float.

The following sections focus on various attributes of AI in the study reach and its evolution, but the separation is purely for convenience. The various attributes are separated because they have different effects on the hydraulics of the Peace River. For example, the spatial extent and thickness of AI affect the amount of ice that can be stored and subsequently released in the form of an AI wave. The AI thickness can change the cross section of the river channel as well as the local slope of the river. The roughness of the bed as AI accretes and releases affects the conveyance of the river channel and the water depth and velocity. However, these observations are all of the same AI and their effects are interrelated.

3.1 Spatial extent of anchor ice

The 2D side scan images lend themselves well to observing the spatial extents of AI as the ledges, where strips and large pieces of AI have detached, are clearly visible (Figure 9). Even in relatively shallow portions of the river that were 1 to 3 m deep, good quality 2D imagery extends beyond the 100 m swath that was recorded. The ledges along the edges of the AI are clearly visible because the ledges facing the sonar give much stronger returns than their relatively flat surroundings, and the back sides of ledges cast long shadows on the river bed beyond.

The evolution of AI is also evident when comparing 2D side scan images from subsequent floats. As an example of this, Figure 9 contains three images of the same location as recorded on February 5, 11 and 12. On February 5, at a higher flow rate and colder air temperatures, this location was completely covered with AI of the same thickness. The evolution of AI ledges between successive floats indicates that AI accretion and release can be highly dynamic and is not necessarily a complete cycle of daily accretion and release.

In many cases, thicker AI produced acoustic returns of equal or higher magnitude as compared to adjacent, thinner layers. Figure 10 shows an example of this predominant case. This is consistent with Kerr, et al (2002) and their description of how AI initially forms around individual bed features but later can evolve to a contiguous mat. However, an example showing the opposite was found on February 7 and is shown in Figure 11. This could be due to changing flow characteristics at this location since the river flow was reduced at the Peace Canyon dam between the floats on February 5 and 7.

These observations suggest that, if flow characteristics are changing as AI accretes and grows, there could be weaker or more permeable layers within an otherwise contiguous AI feature. Some of these variations within a contiguous AI feature could be more susceptible to failure as hydraulic and thermodynamic conditions change, and this failure could result in partial AI release. An analogy is a snowpack with weak layers of snow that can fail and result in avalanches.

AI ledges and contiguous AI mats were found everywhere along the 13 km long by 100 m wide data sets on all four floats in February. More work needs to be done to distinguish between images of the gravel river bed that are covered by AI, and those that are not, to quantify fractional area AI coverage. However, visual inspection of the images indicates that fractional coverage is definitely more than 50% and could be as high as 90 – 100% in some reaches. The imagery obtained offers direct confirmation that anchor ice can occur in very large quantities on the bed of a large river, which was only indirectly quantified in previous studies (Jasek, 2016).

3.2 Transverse anchor ice ledges

A reach of river where transverse AI ledges commonly formed (Figure 12) is located at about the midpoint of the 13 km float trips (Figure 3). This reach has a shallow gravel bar present across the entire river width and the water velocity in this reach was accelerating as the depth became shallower. The gravel bar can be seen in Figure 3. All the transverse ledges that were observed occurred on the upslope side of the gravel bar as shown in Figure 5. The locations of the vertical lines in this figure were calculated from geographical coordinates of the ledges at the centre of the swath in the 2D side scan imagery and coincided with drops in bed elevation (0.2 to 0.3 m) as calculated from the 3D side scan data. The ledges changed location within a 100 m range between floats and there was a second transverse ledge present about 200 m further upstream on February 11. It is difficult to determine the direction of migration of these ledges and perhaps correlate them with air temperature because floats did not occur every single day. However, from the two floats on February 11 and 12, it appears that the ledge migrated upstream during this time when the weather was warming and water was transitioning from supercooled to slightly above freezing. The fact that these transverse AI ledges consistently form on the upstream side of the gravel bar indicates that the velocity and turbulent field present near this type of river bed geometry is conducive to anchor ice growth.

The changes in bed elevation between floats as shown in Figure 5 would not be accurate enough to derive changes in AI thickness between floats due to uncertainties arising from GPS inaccuracies and water surface elevation determination. The latter was linearly interpolated from surveyed water levels at the upstream and downstream ends of the 13 km float trips. The bed profile in Figure 5 was determined by the PingDSP software and was calculated from the average depth taken from bottom returns over a 35 or 70 degree lateral swath (depending on data quality). This means that, because the river was 2 to 6 m deep, the bed profile was calculated from a swath of bottom returns 1.3 to 8.4 m wide in the middle of the 100 m wide swath of sonar data. The elevations are calculated by taking the interpolated water level elevation and subtracting the PingDSP depth and the sensor submergence, which was measured using a tape measure.

The depths in Figure 5 diverge dramatically between distance 7800 and 8600 m. It is believed that this is not due to AI differences (AI ledges of this magnitude were not measured), but due to very rapidly varying river bed geometry in this reach where slight differences in float paths yielded very different depths. After the 8600 m mark, the depths were similar again where presumably the channel depth in the transverse direction became more uniform.

3.3 Longitudinal anchor ice ledges

Some reaches of the 13 km float often showed longitudinal AI ledges as shown in Figure 13. One of these locations is indicated on Figure 3. Each image shows a 320 m by 100 m portion of the river bed and the last image on March 15 is AI free. Boulders are prominent on the right side of each image, close to the right bank. The same boulders in each image can be used for more accurate reference positioning of the AI ledges. From these images, it appears that the right side of the river has thicker and longer duration AI, possibly because it is shaded by steep river banks on the south side of the river channel and/or because the shallower portions of the river were more conducive to AI growth. Multiple ledges are apparent in the February 11 image indicating that weak horizontal layers of anchor ice can cause partial detachment from the bed.

3.4 Roughness of anchor ice

The river stage and water and air temperatures shown in Figures 3 and 4 were collected 1.5 km downstream of the Dunvegan highway bridge. The images presented in Figure 14 were obtained at the same location. These images show multiple layers of AI on both the February 5 and 12 floats which cause increased roughness as well as an increase in bed elevation. An ice-free image from March 15 is presented for comparison, showing the ice-free river bed being quite smooth. The depth colorization ranges from red to blue over 1.5 m in these images.

3.5 Thickness of anchor ice

Although the sonar instrument is capable of producing survey quality bathymetry, the GPS instrument that was used did not have a corresponding level of accuracy. Therefore calculation of AI thickness was not possible by surveying the same location with and without AI and subtracting the two surfaces. However, the relative accuracy of the sonar data is typically within a centimeter or two, depending on the depth of the river, and some of the islands and ledges of AI that were observed were measured to be 0.15 – 0.8 m high as compared to the surrounding area. This indicates that portions of the AI were at least that thick. The 4 m by 12 m AI island shown in Figure 15 was 0.3 – 0.45 m thicker than the surrounding area while the AI island in Figure 16 measured 0.67 to 0.87 m thicker than the surrounding area. Ice-free images of those same locations are shown for comparison. Figure 17 shows a larger island that is two layers thick and up to 0.6 m thicker than the surrounding area. Figure 15 shows that if the water surface and river bed are not coplanar, colorizing the swath bathymetry data according to depth is not too meaningful. There is just too much variability in river depth as compared to variability in AI thickness. The other figures with AI islands were acquired from flatter portions of river bed. Figure 18 shows several neutrally buoyant pieces of AI that were observed, likely containing enough sediment to counteract the buoyant forces of the ice.

At this time, it is not clear whether river bed particle size or ice texture can be inferred from the sonar data and thereby used to quantify the variation at the scale of hydraulic roughness. A preliminary attempt was made to assess the variability in depths from sonar returns in a sample of AI and a sample of river bed, to infer which surface was rougher, but that analysis has not been completed and is beyond the scope of this paper.

3.6 AI release

On the February 12 float, the water temperature at the sonar was above freezing for the entire float and the air temperature was over 5 °C as shown in Figures 6, 7, and 8. However, the river bed was still widely covered with AI since this was only the second day of relatively warm air temperatures after a prolonged period of cold weather. In Figure 19, a piece of AI was observed neutrally buoyant or rising from the bed of the river. These were visually confirmed (Figures 1e and 1f). The temperature of the water at this point was 0.035 °C. In Figure 19, the same image is presented with both acoustic return strength and depth. The depth range from red to blue is 2 m and the acoustic shadow on the bed below the floating piece of AI is clearly visible. In Figure 20 taken on February 7, it appears that those pieces of AI may have detached from the downstream end of the lower elevation strip due to hydraulic uplifting, which is a process that was photographed and videoed in Jasek et al. (2015).

4. Conclusion and further work

From the first time use of this type of instrument on the Peace River in winter, it can be concluded that 3D side scan sonar can help quantify the presence, thickness, extent, and possibly the roughness of anchor ice. The imagery and bathymetry provides direct confirmation that anchor ice can occur in very large quantities on the bed of a large river. This has important implications for river ice modelling where anchor ice is often neglected.

AI features and continuous AI reaches were found on all four floats trips in February everywhere along the 13 km long by 100 m wide swath of imagery. More work needs to be done to be able to distinguish between images of ice-free gravel river bed and areas of river bed covered by AI, in order to quantify the fractional portion of AI coverage. However, visual inspection of the images indicates that fractional coverage is definitely more than 50% and could be as high as 90 – 100% in some reaches.

Since this was the first winter season that the 3D side scan sonar was deployed, there is much more data that can be collected in future years to gain further understanding of anchor ice processes in the Peace River. One incremental improvement in data collection is to upgrade the GPS equipment so that survey-quality swath bathymetry can be collected both with and without AI to accurately calculate its thickness, independent of river flow and stage. This data could also be used to further understand how much AI releases. For example, does AI release from the bed-ice interface only or can it release from a weak layer within a contiguous AI feature.

Another unique condition in which data could be collected is during episodes of river stage-up that are larger than what was present during the four float trips in February 2017. On those floats, increases in river stage during super cooling did not exceed 0.25 m (Figure 7a). However, in January 2017 during a period of constant high flow (Figure 7c) before the sonar instrument had been purchased, a larger stage increase of up to 0.55 m was observed at the same location during supercooling conditions. This indicates that AI accumulations may have the potential to be rougher and/or thicker than what was observed on the floats in February. Collecting sonar data under these conditions could help explain why increases in river stage on the Peace River can sometimes exceed 0.5 m, and even remain constant for several days, when at other times the river stage fluctuates diurnally and never really exceeds 0.25 m. Is the ice at the gauge location really that thick or extra rough or might there be an AI dam forming downstream? A combination thereof may also be possible.

Two other questions that arose during data collection and analysis are:

1. Can layers of different types of AI occur within one AI deposit, i.e. from varying flow or thermal conditions? If these layers exist, can they have differing strengths or can they be more susceptible to melt or mechanical separation than other portions of the same AI feature?
2. To what extent does solar radiation influence the temperature within the water column and how much of that warm water mixes down to the AI? For example, three quarters of the way through the float on February 7, above freezing water temperatures were recorded even though incoming water was supercooled and the air temperature was well below 0 °C. And how might that warm water affect AI growth and release?

Acknowledgments
The authors would like to thank Monica Paslawski with Timberoot Environmental who assisted with several floats. Also, the timely help and response from staff members at PingDSP while their 3D side scan sonar instrument was being set up and used was greatly appreciated. They also provided expertise and several software enhancements to assist with data analysis. The authors would also like to acknowledge Rescue Canada for giving them the training and knowledge to work safely in the freezing river conditions. Thank you to the Town of Fairview for permitting the use of their water intake buildings for placement of barometric loggers, and for providing access to exit the river. Finally, the authors wish to express their gratitude to Dunvegan Gardens who provided a storage area for the boat and trailer in between float trips.

References

Beltaos, S., Malenchak, J., Clark, S., 2013. *River Ice Formation.*: Chapter 5 Anchor Ice. Pub. by CGU-HS Committee on River Ice Processes and the Environment, Edmonton, AB, pp 135-157.

Jasek, M., Shen, H.T., Pan, J., Paslawski, K., 2015. Anchor Ice Waves and their Impact on Winter Ice Cover Stability. Proc. 18th CGU-HS CRIPE Workshop on the Hydraulics of Ice Covered Rivers, Quebec City, QC.

Jasek, M,. 2016. Investigations of anchor ice formation and release waves. Proc. 23rd IAHR International Symposium on Ice. Ann Arbor, Michigan USA.

Kerr, D.J., Shen, H.T., Daly, S.F., 2002. Evolution and hydraulic resistance of anchor ice on gravel bed. Cold Regions Science and Technology, 35(2): 101-114.

Marko, J.R, Jasek, M., Topham, D.R., 2017. Technical Report: In Situ Anchor Ice, Frazil and River Ice Cover Development: Perspectives from Acoustic Profile Studies. ASL Environmental Sciences Inc.

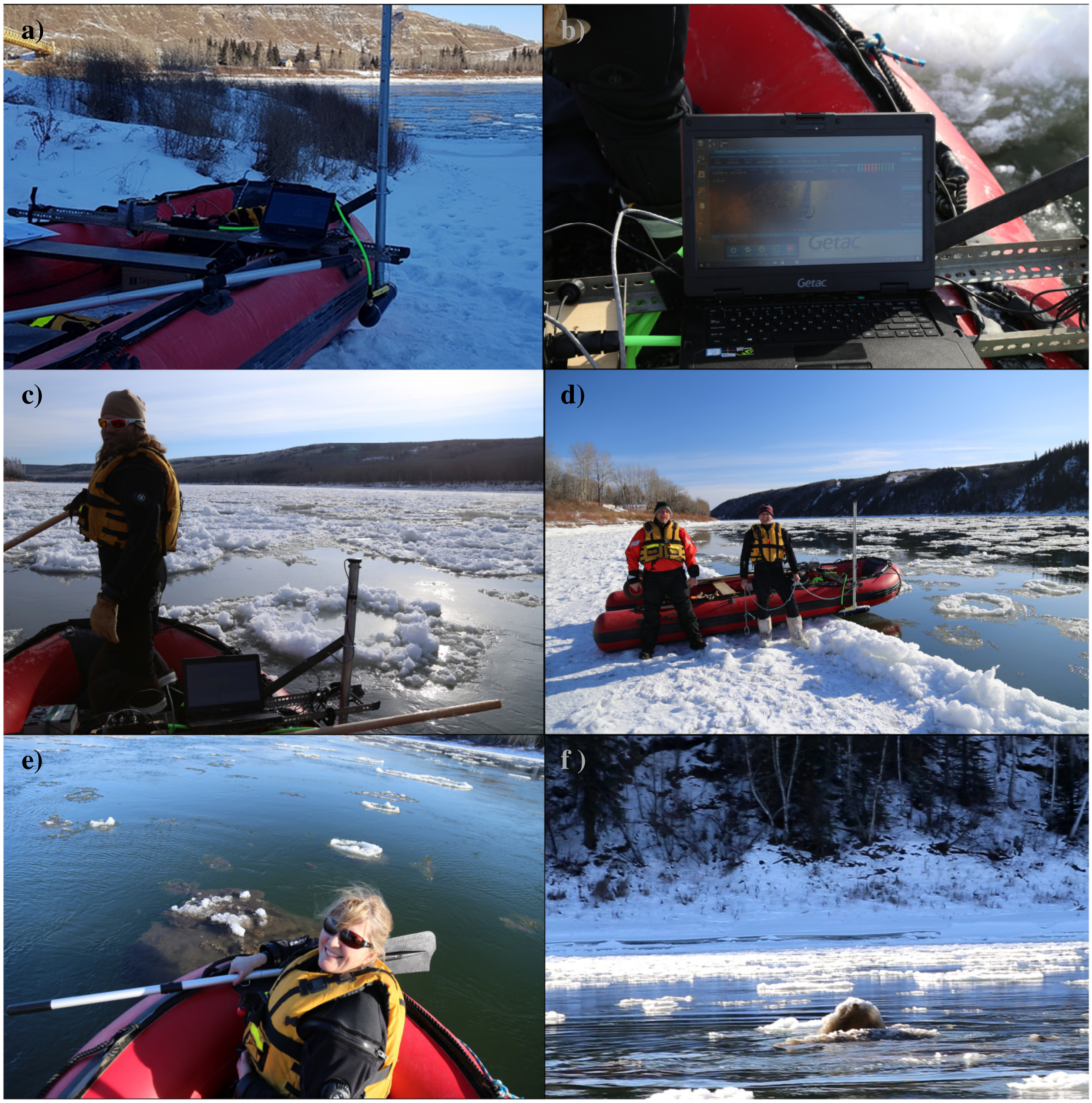

Figure 1. a) Boat, pole-mounted 3D side scan sonar, and temperature probe, b) real-time bed bathymetry display, c) ice conditions during float trip on February 7, d) ice conditions during float trip on February 12, e) newly released anchor ice on February 12, f) a video frame showing the release of anchor ice on February 12.

Figure 2. Location of the study reach of the Peace River.

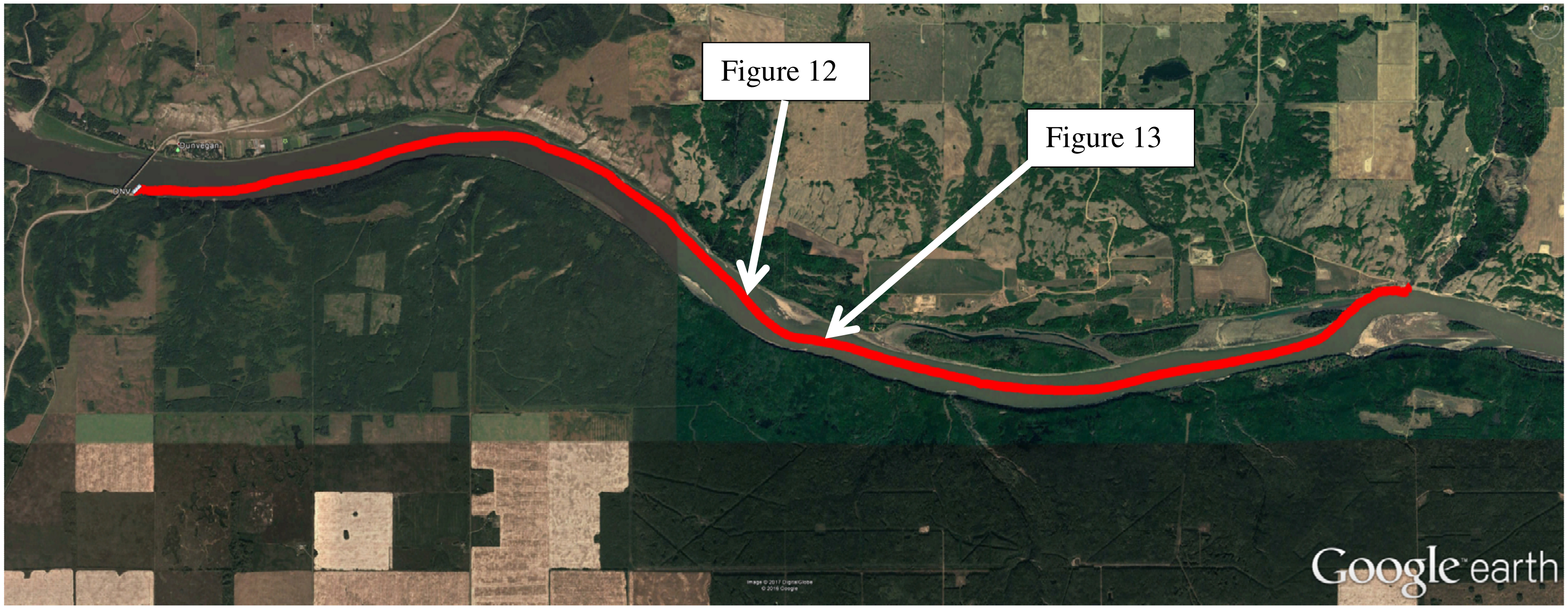

Figure 3. 13 km long GPS track and 100 m wide swath covered by 3D side scan sonar.

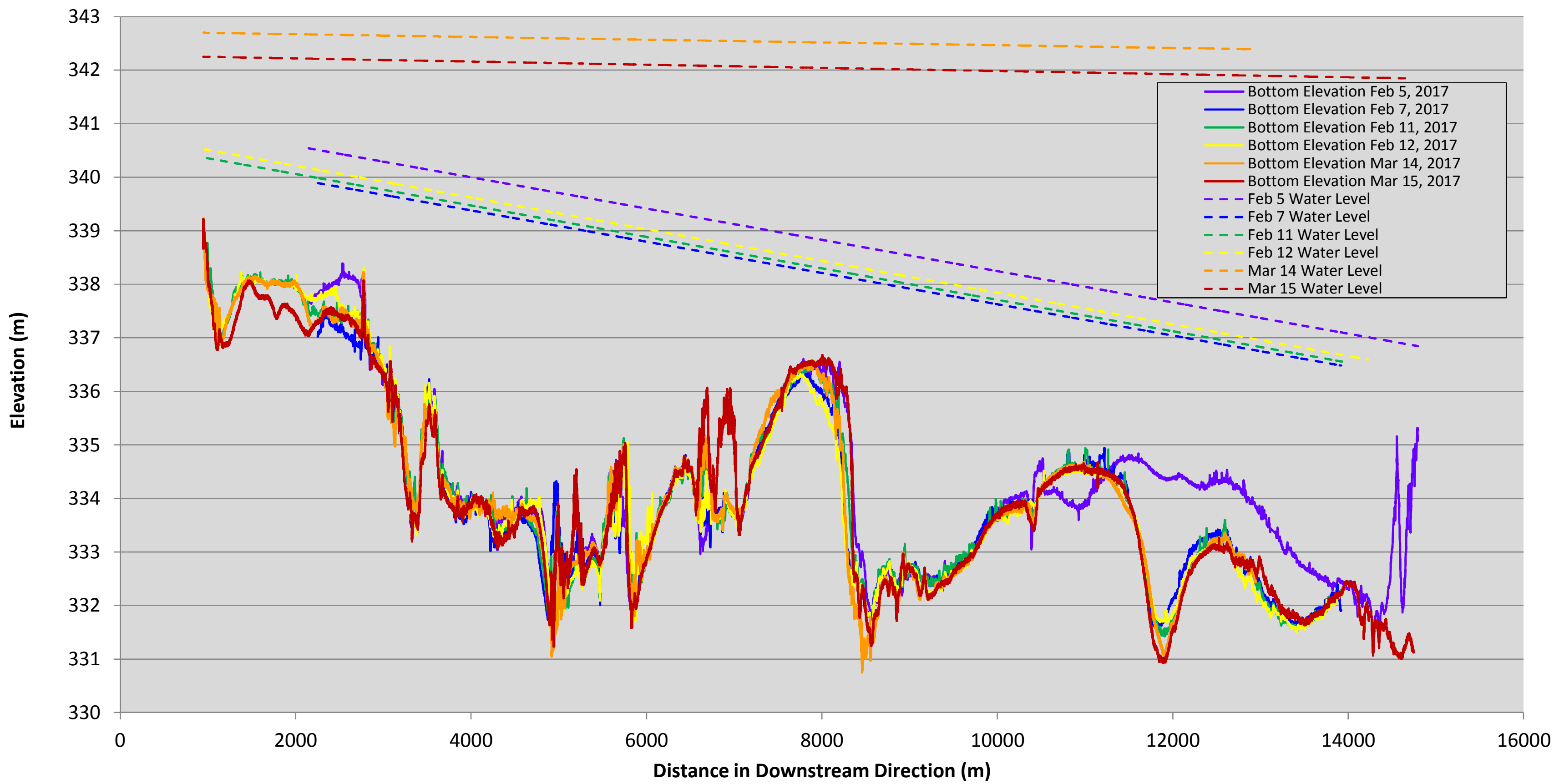

Figure 4. Bed and water surface elevations during the six float trips. The water surface elevations were linearly interpolated from surveyed water levels at the upstream and downstream extremes of the float trips. The bed elevations were determined by subtracting the PingDSP computed depth and instrument submergence from the interpolated water surface elevation.

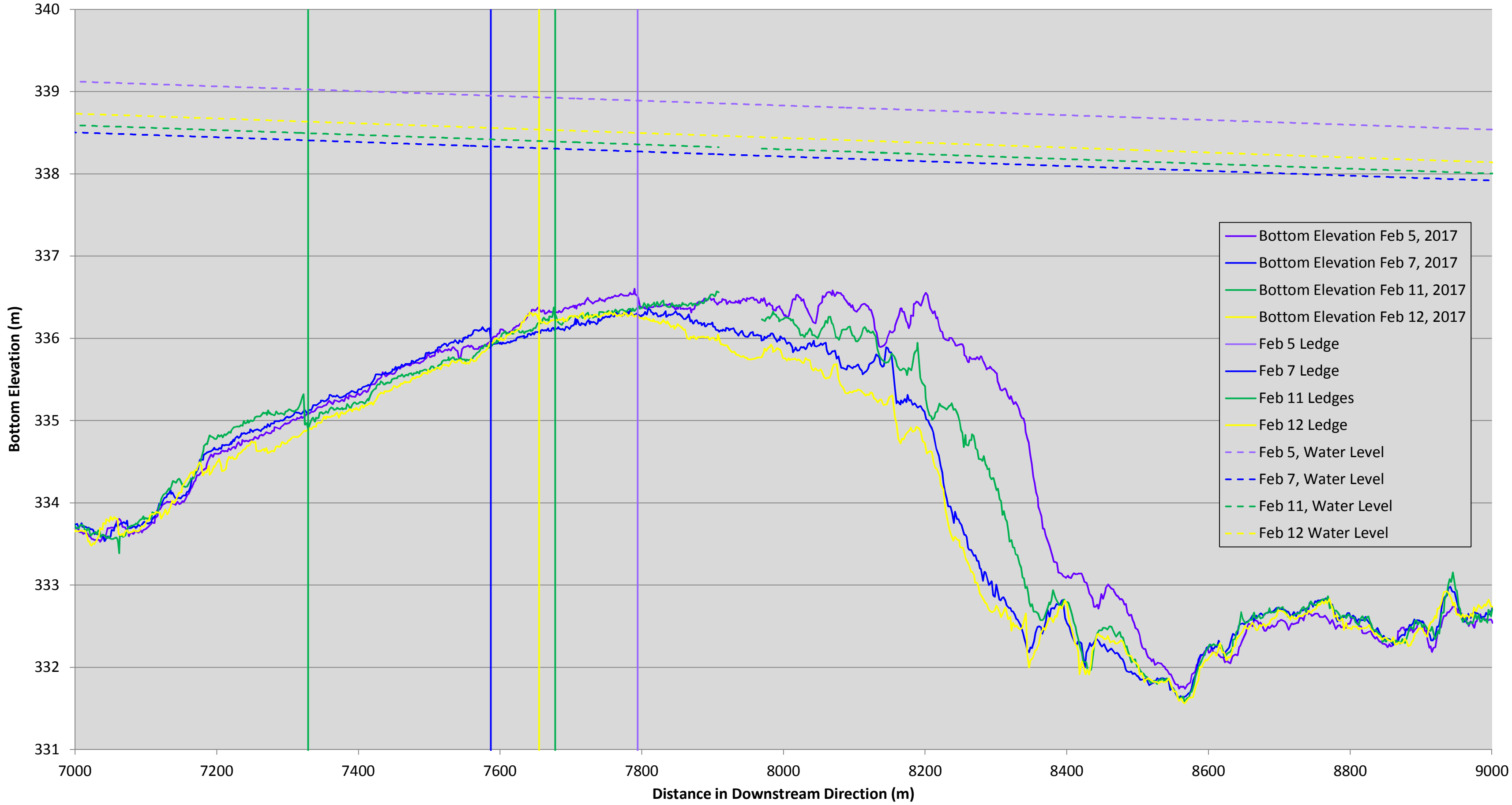

Figure 5. River bottom profiles computed from PingDSP signal and surveyed water surface profile for the February 5, 7, 11 and 12 float trips in a river reach with transverse AI ledges. The locations of the AI ledges (from Figure 16) are shown as vertical lines. The water levels were linearly interpolated from surveyed water levels from the upstream and downstream reaches of the float trips.

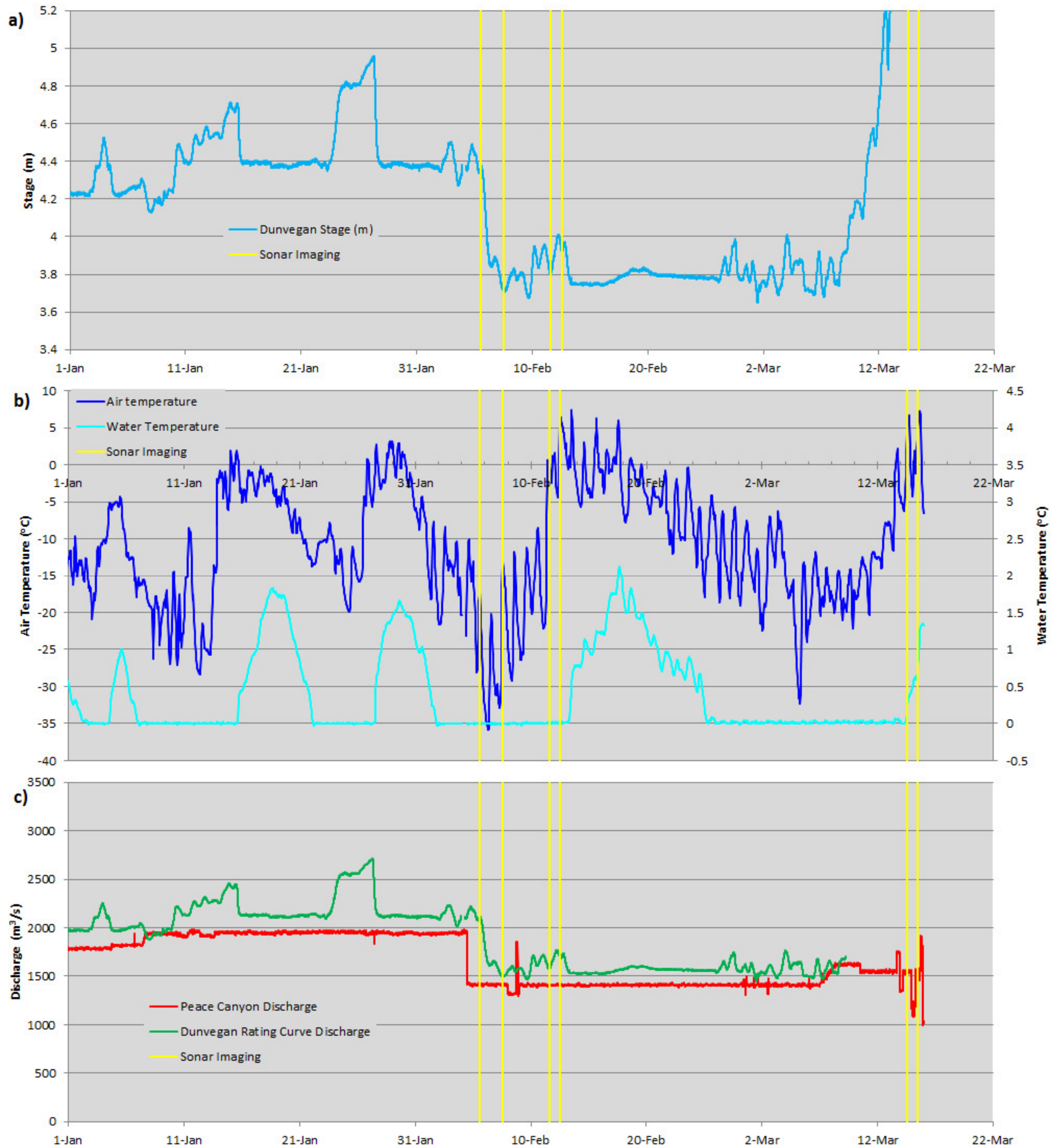

Figure 6. Graphs of a) river stage and b) air and water temperature as measured at the Dunvegan highway bridge where sonar data collection began, c)upstream discharge measured at the Peace Canyon dam 300 km upstream and discharge computed from the stage-discharge curve at Dunvegan. Sonar imaging dates are plotted as yellow lines.

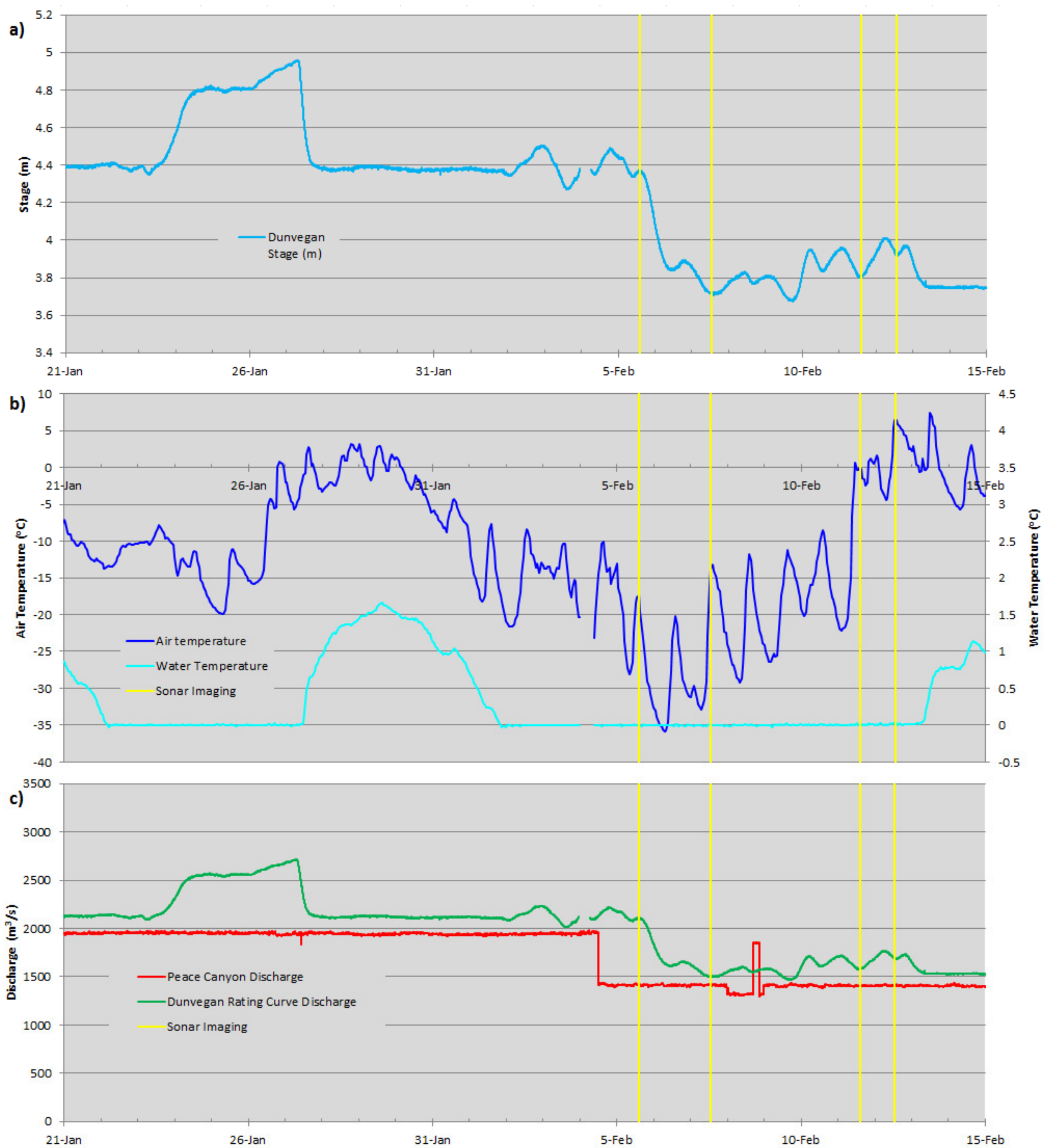

Figure 7. Graphs of a) river stage and b) air and water temperature as measured at the Dunvegan highway bridge where sonar data collection began, c) upstream discharge measured at the Peace Canyon dam 300 km upstream and discharge computed from the stage-discharge curve at Dunvegan. Sonar imaging dates are plotted as yellow lines.

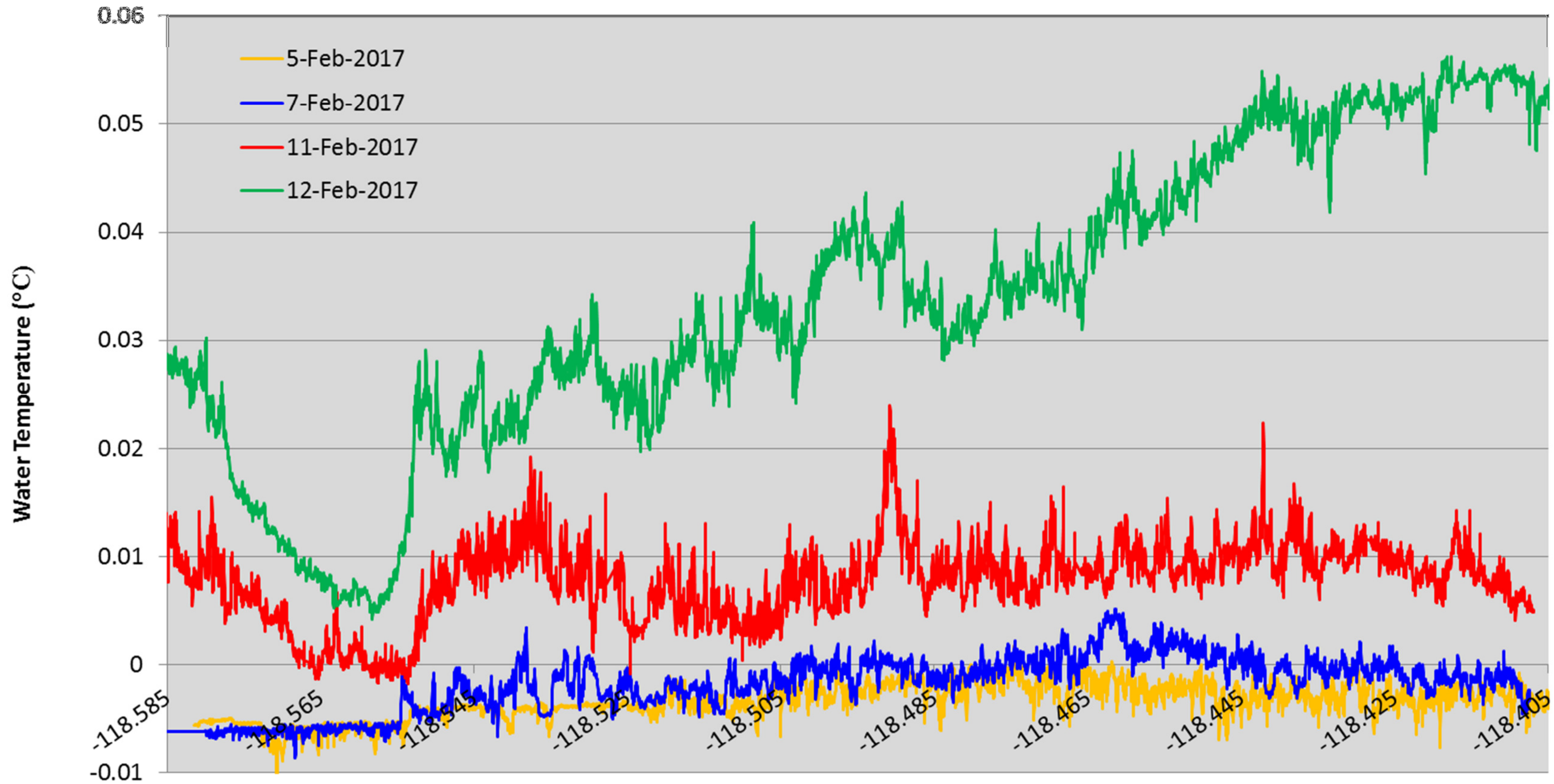

Figure 8. Water temperatures at the sonar instrument during the first four floats.

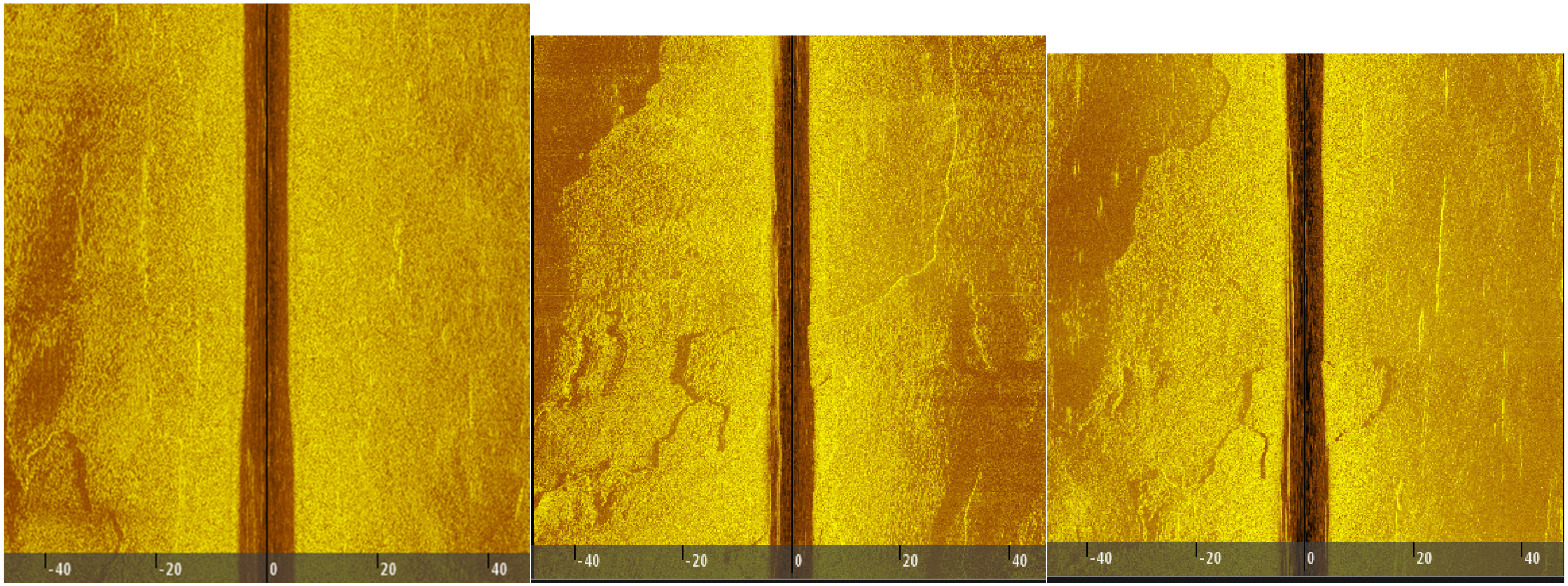

Figure 9. An evolving AI ledge on February 5 (left), 11 (center), and 12 (right). Downstream direction is bottom to top.

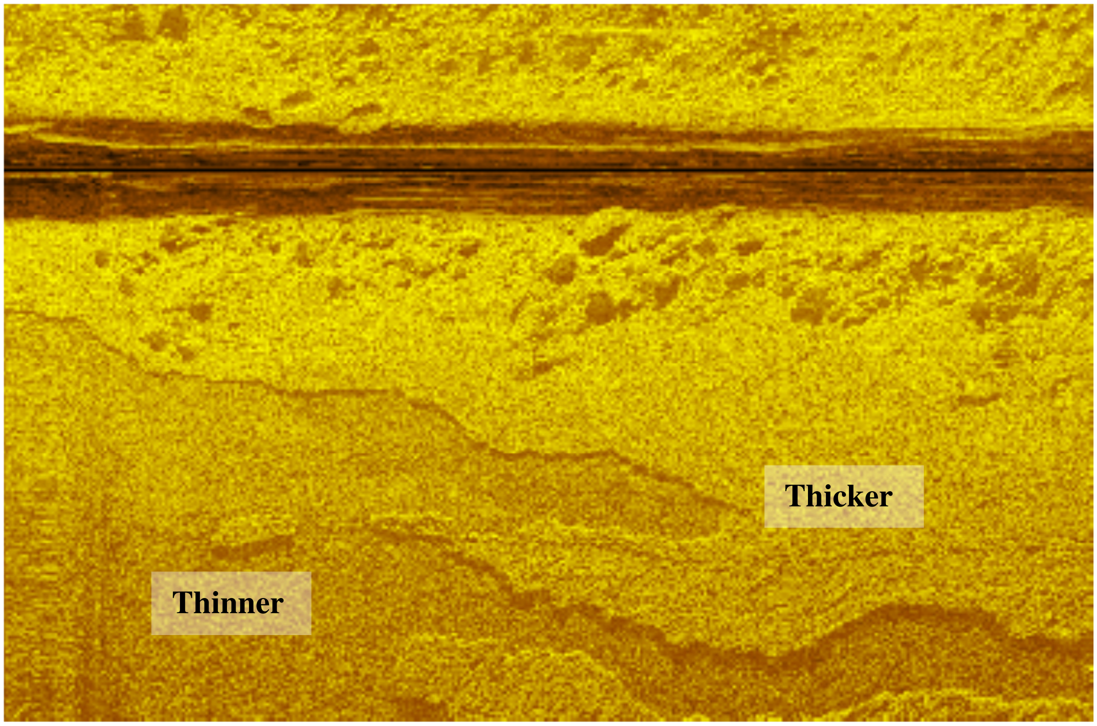

Figure 10. A typical example of high sonar return strength coming from thicker AI. Flow direction is left to right. February 11.

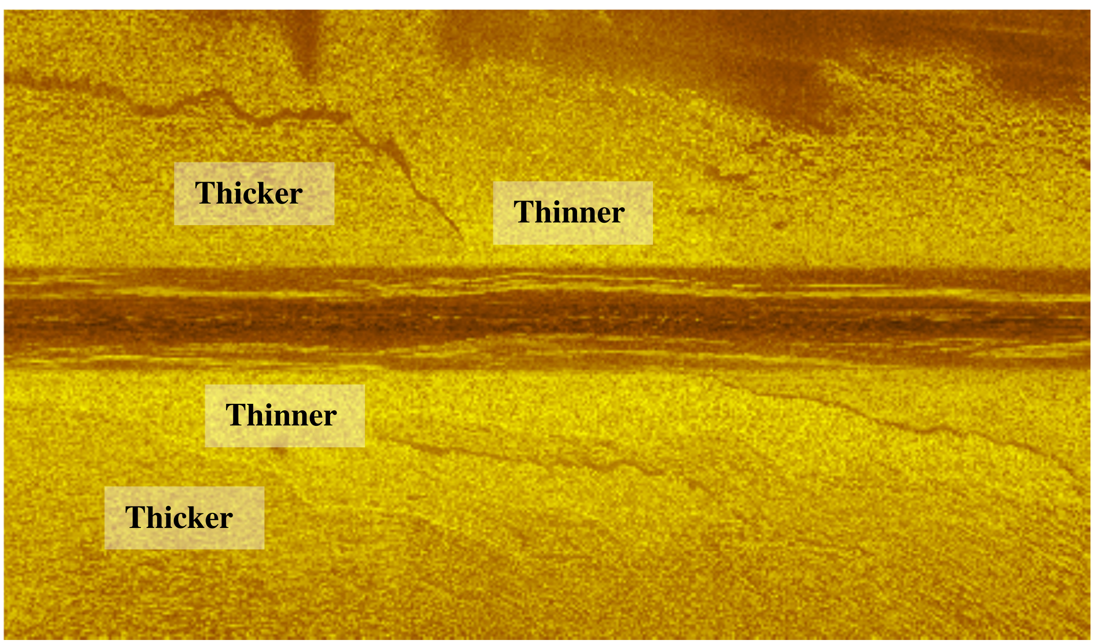

Figure 11. A relatively unique example of high sonar return strength coming from thinner AI. Flow direction is left to right. February 7.

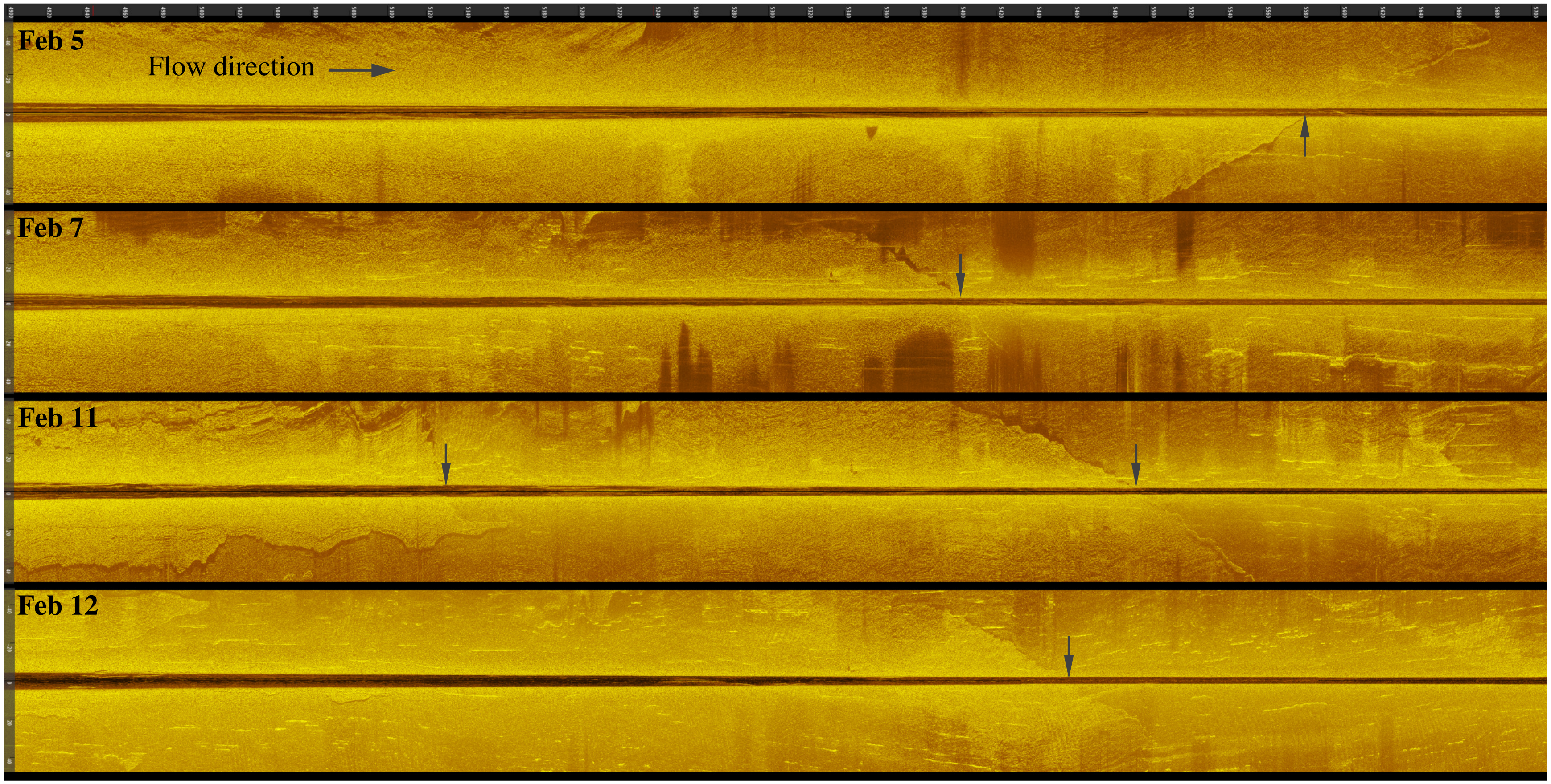

Figure 12. Transverse AI ledges (vertical arrows) shown on 800 m by 100 m wide 2D side scan images for the same river reach on February 5, 7, 11 and 12. There are two transverse AI ledges in the February 11 image as well as some longitudinal ledges at the left side of the image. The large dark areas are occurrences were the acoustic beam is blocked by surface ice floes close to the sensor and the thin bright bands are acoustic returns from surface ice and mid-water ice targets.

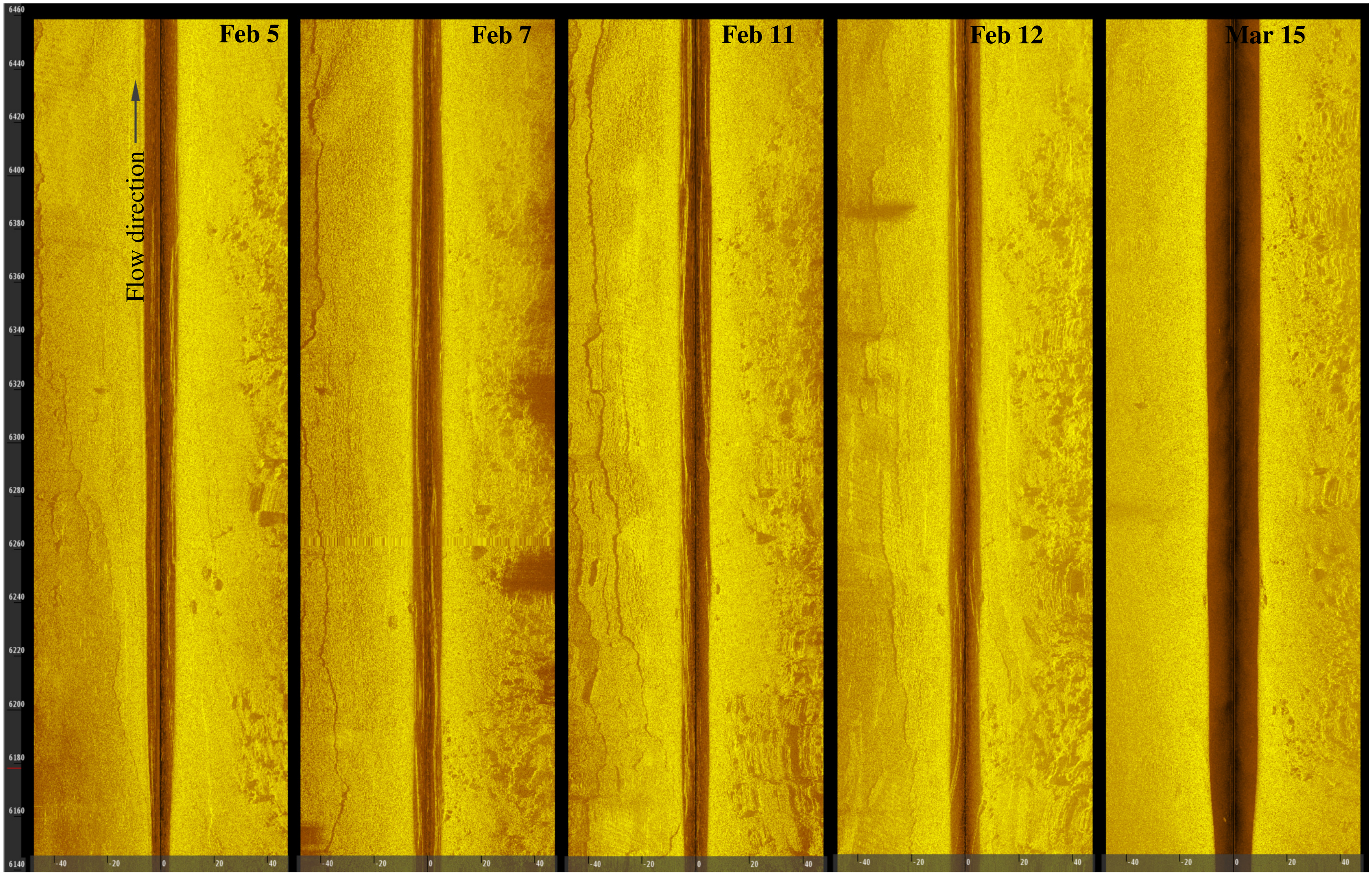

Figure 13. Longitudinal anchor ice ledges shown on 320 m by 100 m wide 2D side scan images for the same river reach on February 5, 7, 11, 12. The March 15 image is anchor ice free as the water temperature was well above freezing. Boulders on the right of each image are close to the right bank on the south side of the river and can be used to reference the locations of AI ledges.

a)

b)

c)

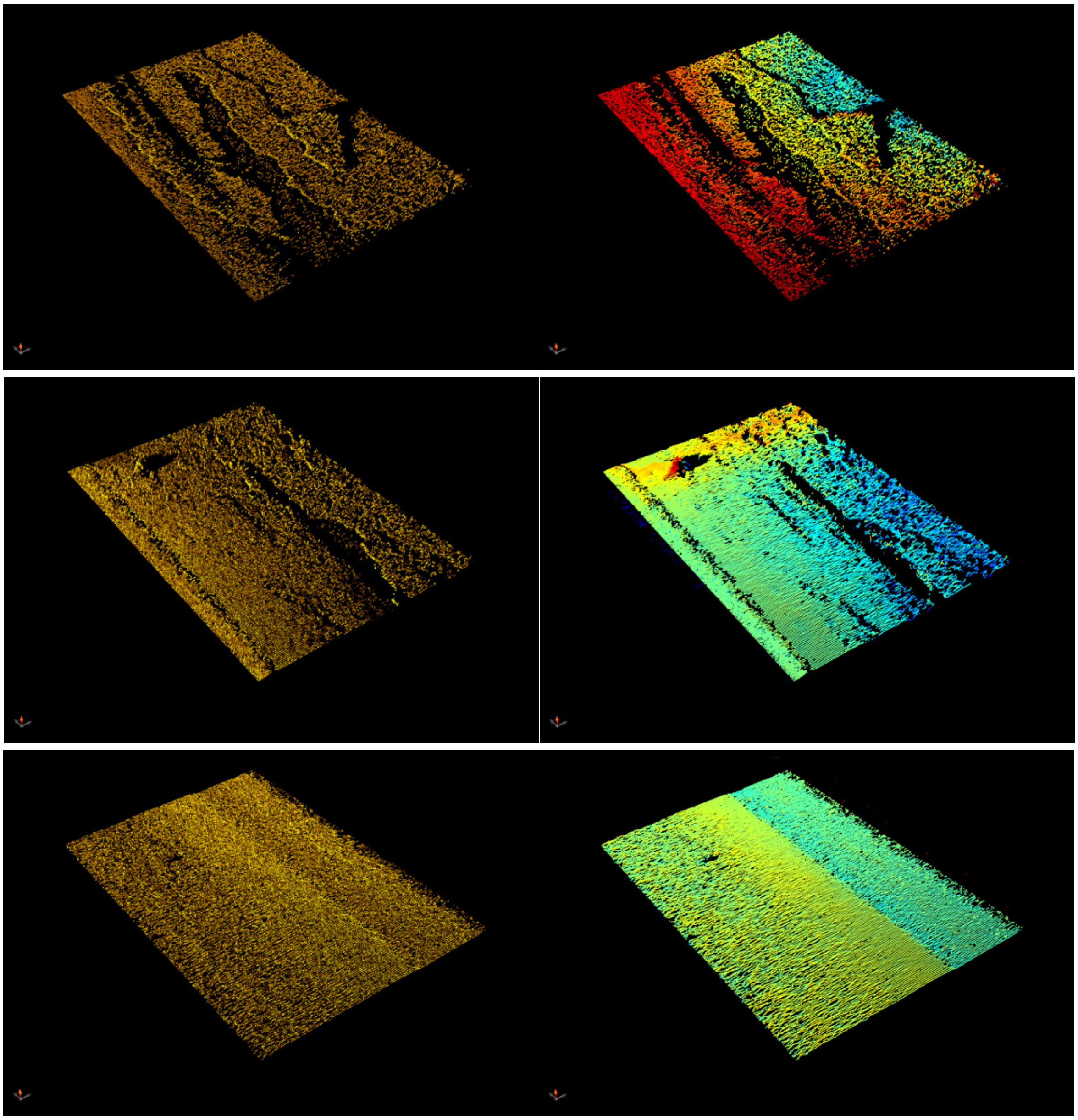

Figure 14. A 20m by 30m portion of river bed on a) February 5, b) February 12, and c) March 15. The depth colorization is 1.5 m from red to blue in the right-side images. Downstream direction is to upper left.

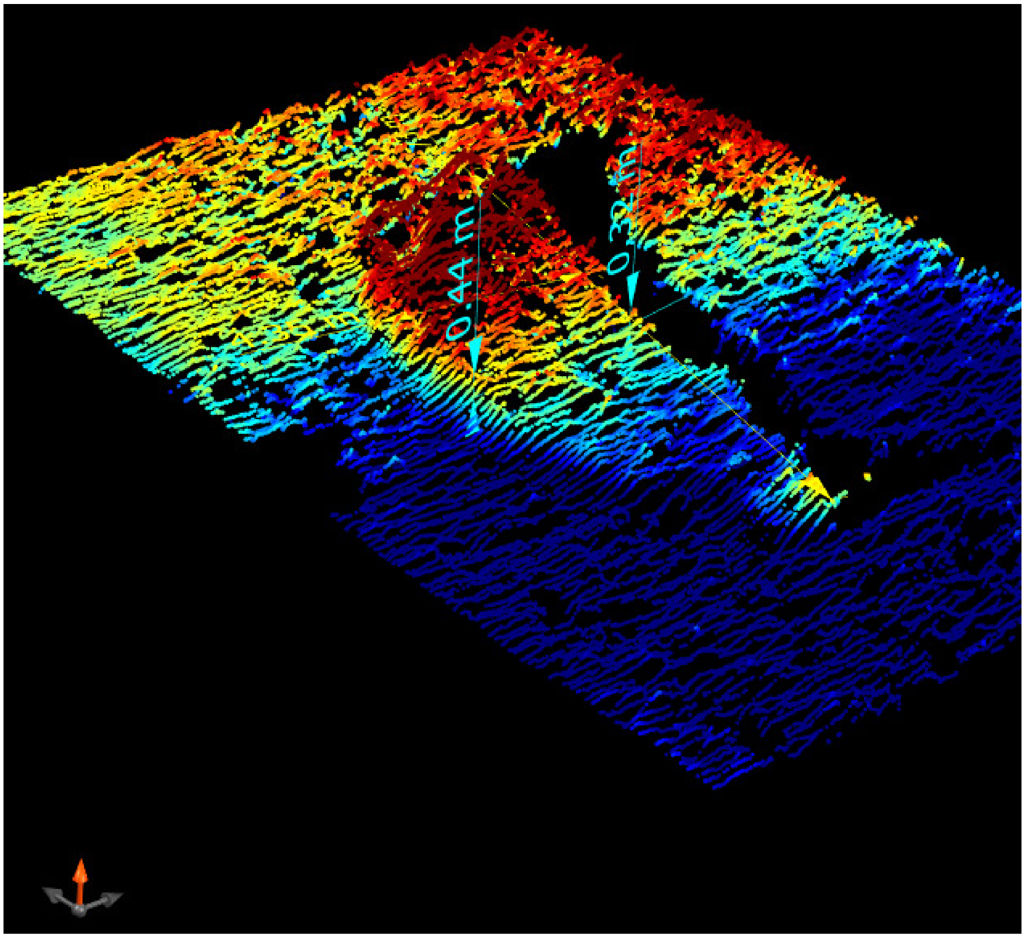

Figure 15. An island of AI 0.3 to 0.45 m thick on February 12. Downstream direction is to upper left.

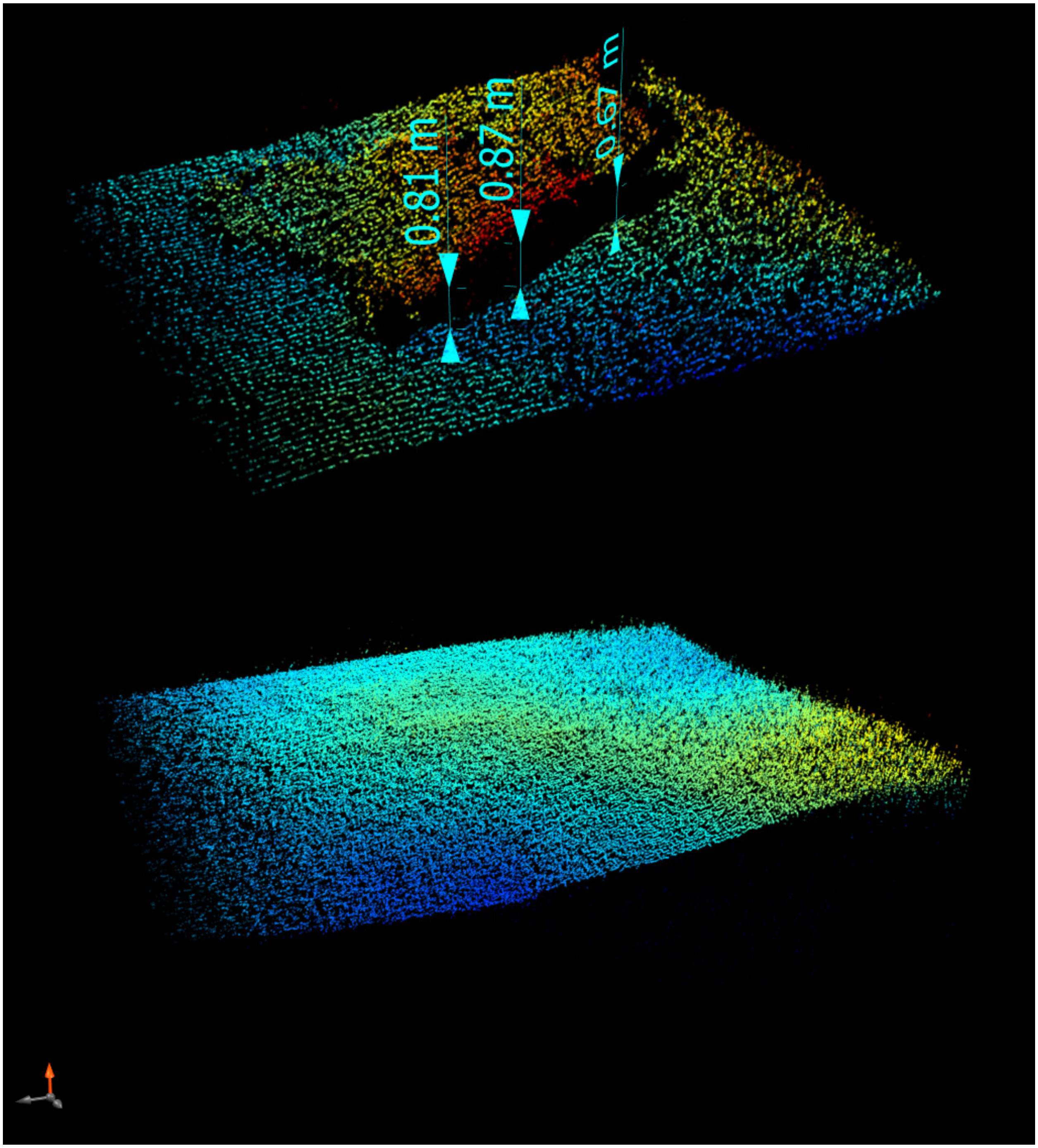

Figure 16. A small AI island over 0.8 m thick on February 7 and the same location ice-free on March 15. Downstream direction is to the bottom right.

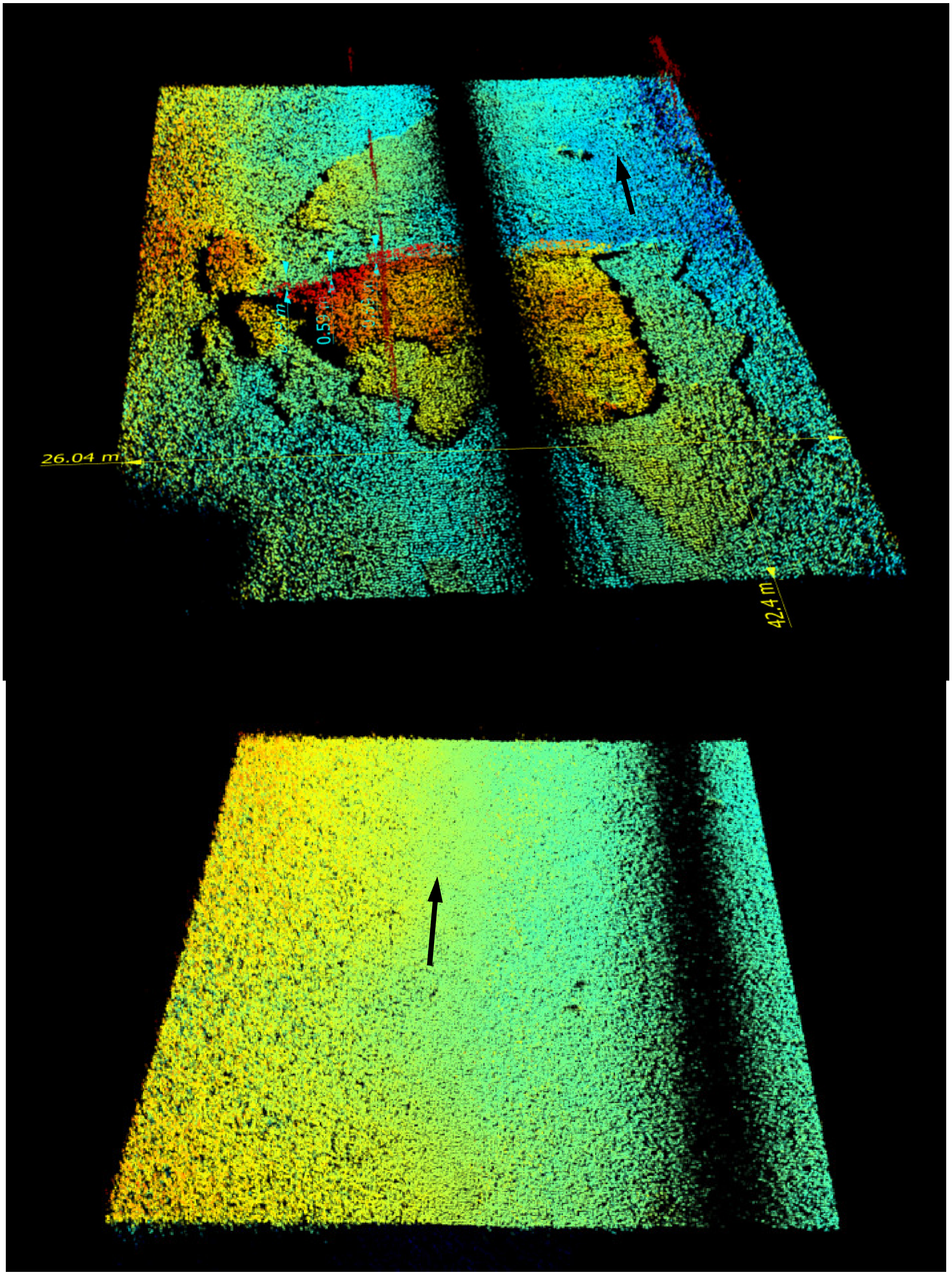

Figure 17. Multiple levels of AI on February 7, up to 0.6 m thick, and the same location ice-free on March 15.

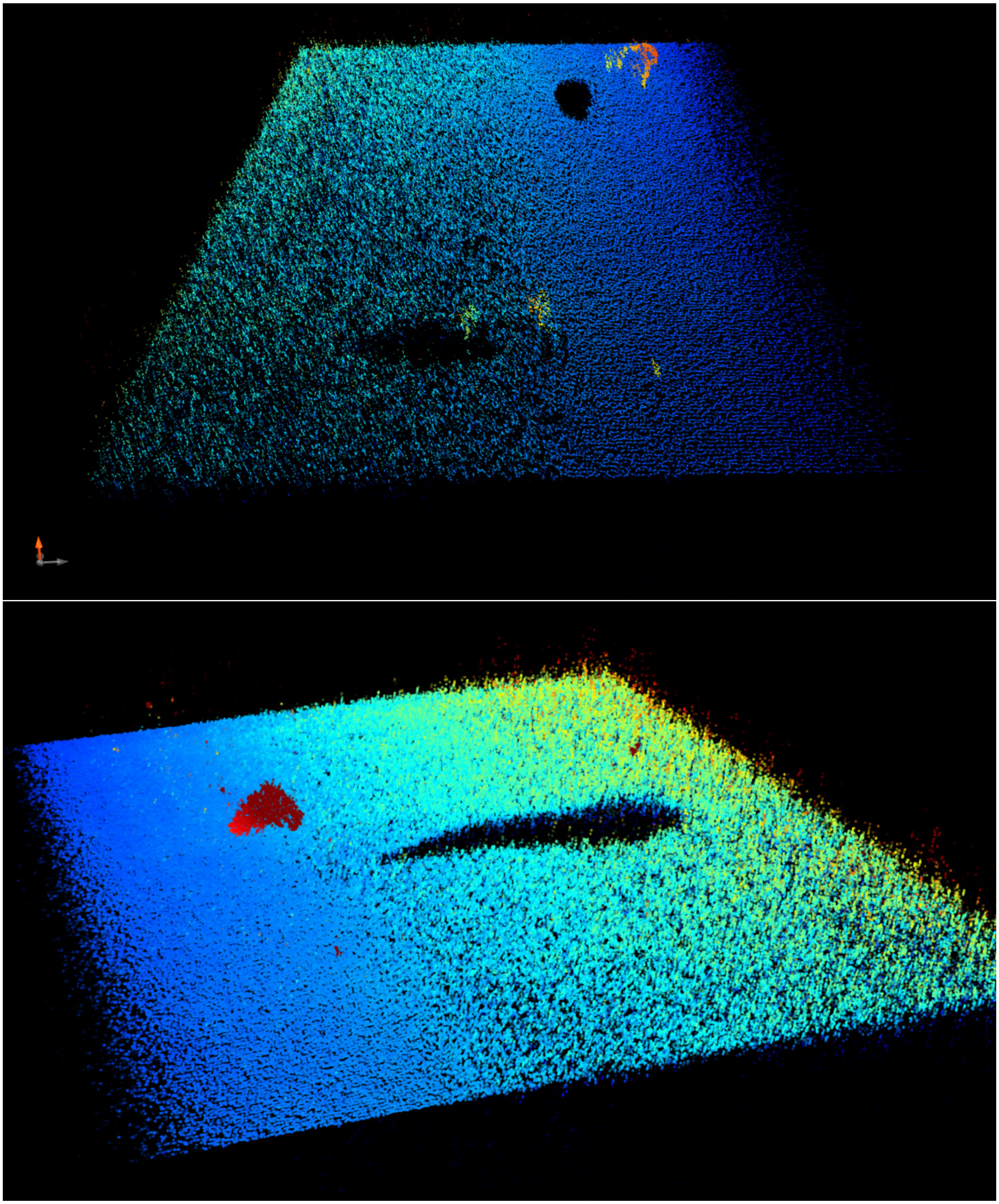

Figure 18. Neutrally buoyant AI and their shadows on February 12.
Looking downstream.

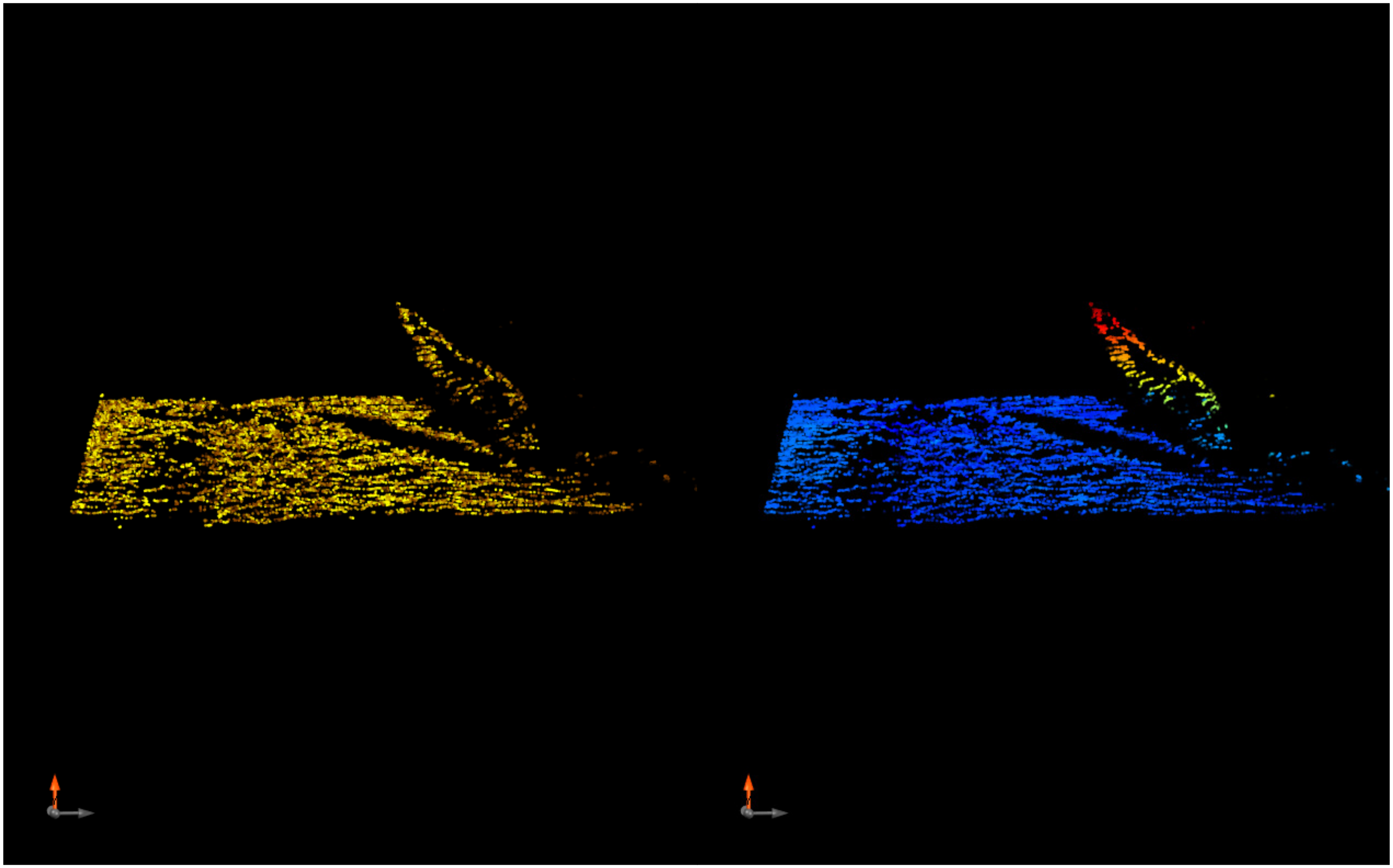

Figure 19. A piece of AI on February 12 that was recorded floating above, or rising from, the bed of the river. The depth colorization is 2 m from red to blue in the right image. Looking downstream.

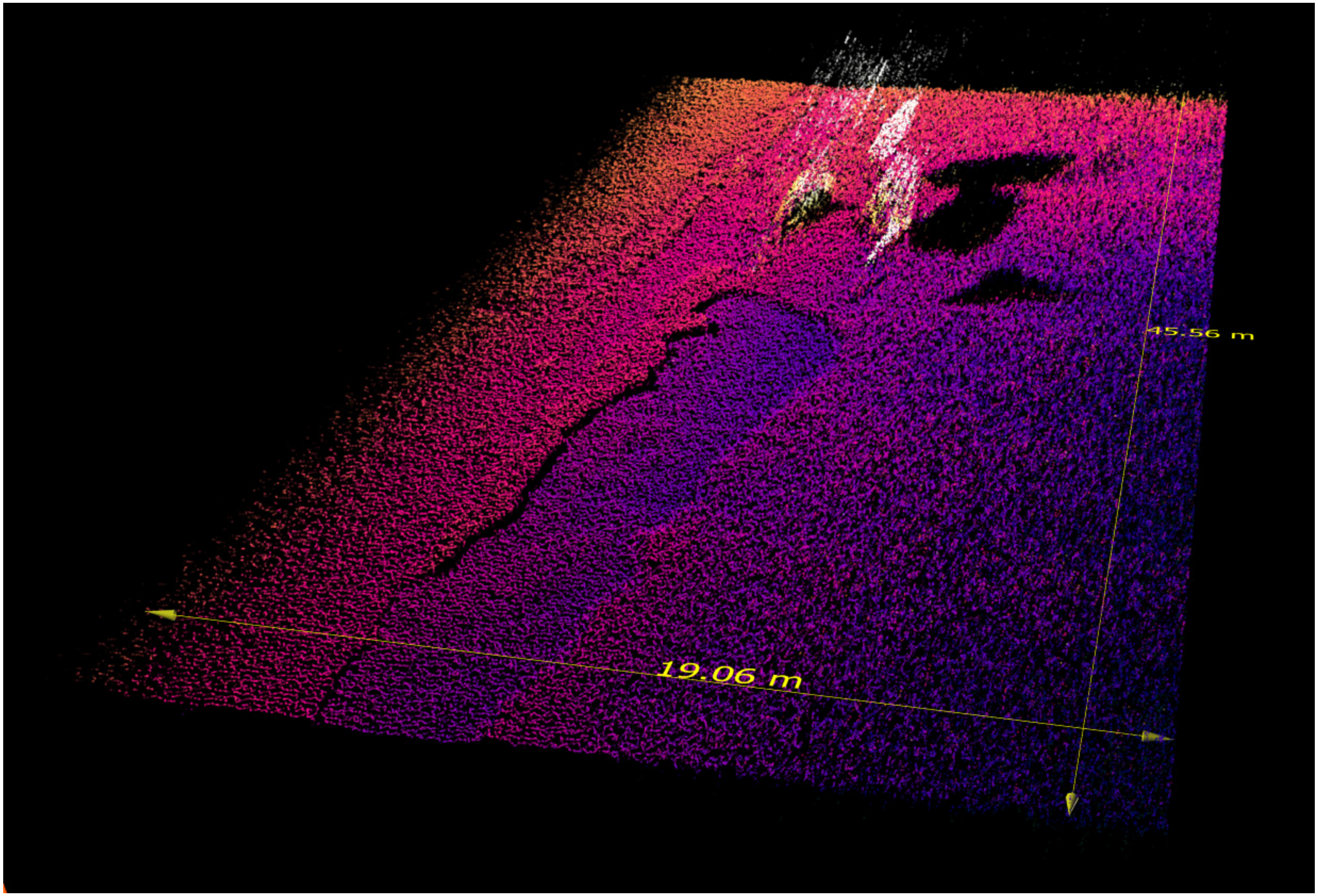

Figure 20. Several pieces of AI in the water column on February 7, appearing to have just recently detached. Their acoustic shadows are clearly visible on the in-situ AI beyond them. Image is oriented looking downstream and the pieces of AI may have detached from the downstream end of the lower elevation strip shown in dark purple.